

# Color Superconductivity and Chiral Symmetry Restoration at Nonzero Baryon Density and Temperature\*

Jürgen Berges and Krishna Rajagopal<sup>†</sup>

*Center for Theoretical Physics  
Laboratory for Nuclear Science  
and Department of Physics  
Massachusetts Institute of Technology  
Cambridge, Massachusetts 02139*

(MIT-CTP-2725, hep-ph/9804233)

## Abstract

We explore the phase diagram of strongly interacting matter as a function of temperature and baryon number density, using a class of models for two-flavor QCD in which the interaction between quarks is modelled by that induced by instantons. Our treatment allows us to investigate the possible simultaneous formation of condensates in the conventional quark–anti-quark channel (breaking chiral symmetry) and in a quark–quark channel leading to color superconductivity: the spontaneous breaking of color symmetry via the formation of quark Cooper pairs. At low temperatures, chiral symmetry restoration occurs via a first order transition between a phase with low (or zero) baryon density and a high density color superconducting phase. We find color superconductivity in the high density phase for temperatures less than of order tens to 100 MeV, and find coexisting  $\langle qq \rangle$  and  $\langle \bar{q}q \rangle$  condensates in this phase in the presence of a current quark mass. At high temperatures, the chiral phase transition is second order in the chiral limit and is a smooth crossover for nonzero current quark mass. A tricritical point separates the first order transition at high densities from the second order transition at high temperatures. In the presence of a current quark mass this tricritical point becomes a second order phase transition with Ising model exponents, suggesting that a long correlation length may develop in heavy ion collisions in which the phase transition is traversed at the appropriate density.

---

<sup>†</sup>Email addresses: [berges@ctp.mit.edu](mailto:berges@ctp.mit.edu) and [krishna@ctp.mit.edu](mailto:krishna@ctp.mit.edu)

\*This work is supported in part by funds provided by the U.S. Department of Energy (D.O.E.) under cooperative research agreement # DE-FC02-94ER40818.

## I. INTRODUCTION

Strongly interacting matter is expected to undergo a phase transition or crossover to a quark–gluon plasma phase both at high temperature and at high baryon density. Since QCD is asymptotically free, when either the temperature  $T$  or the Fermi momentum  $p_F$  is high the effective coupling for typical scattering processes with momentum transfer of order  $T$  or  $p_F$  is small, and one therefore expects a new phase of matter in which color is screened rather than confined and chiral symmetry is restored. The exploration of the phase diagram is of fundamental interest and has applications in cosmology, in the astrophysics of neutron stars and in the physics of heavy ion collisions. The zero density, high temperature axis of the phase diagram is much better explored than the zero temperature, high density axis, since lattice Monte Carlo techniques are well-suited to nonzero temperature but not so well-suited to nonzero chemical potential. Recent work [1,2] suggests a rich phase structure at nonzero density. First, chiral symmetry restoration proceeds via a first order phase transition and ordinary nuclear matter may be described as being in the mixed phase of this transition [1]. Second, above the transition, the quarks may be weakly coupled but the phase they are in is *not* the trivial one. Even at weak coupling, any attractive quark-quark interaction leads to the formation of a condensate of Cooper pairs, which spontaneously breaks color symmetry. Color superconductivity has been studied using perturbative methods valid at asymptotically high density [3], and in a one-flavor model [4]. The authors of Refs. [1,2] have used a model in which the interaction between quarks in two-flavor QCD is modelled by that induced by instantons [6] to estimate the magnitude of the diquark condensate in the phase in which chiral symmetry is restored. We first generalize the variational methods of [1] to a formalism in which we derive a bosonic effective action for the degrees of freedom which condense.<sup>1</sup> For the present investigation, we evaluate the effective action using a mean field approximation. Using the method we describe here, we can analyze circumstances in which a chiral symmetry breaking  $\langle\bar{\psi}\psi\rangle$  condensate and a color breaking  $\langle\psi\psi\rangle$  condensate coexist. Furthermore, we introduce nonzero temperature and current quark mass. In this paper, therefore, we are able to explore the phase diagram as a function of temperature, density or chemical potential, and quark mass.

The phase diagram which we uncover has striking qualitative features, several of which we expect to generalize beyond the model which we consider and to provide a good guide to the physics of two-flavor QCD. At low temperatures, chiral symmetry restoration occurs via a first order phase transition between a phase with low (or zero) baryon density and a high density phase with a condensate of quark–quark Cooper pairs in color antitriplet, Lorentz scalar, isospin singlet states.<sup>2</sup> We find color superconductivity at temperatures  $T < T_c^\Delta$  where  $T_c^\Delta$  is of order tens to almost one hundred MeV, and at most a factor of four higher if we allow interactions other than that induced by instantons. This suggests that color superconductivity may arise in heavy ion collisions, in which the necessary densities

---

<sup>1</sup>Diquark condensation has also been sought in the vacuum using similar methods [5].

<sup>2</sup>There are also indications [1] of a color **6**, Lorentz axial vector, isospin singlet condensate which is many orders of magnitude smaller than the condensates we treat.

are likely accompanied by temperatures of order 100 MeV. The transition we find at  $T_c^\Delta$  is second order for the present model, but the order of this transition may change once gauge field fluctuations are taken into account. We study the competition between chiral and superconductor condensates, in particular when the current quark mass is nonzero and both coexist. For small quark mass, we find that the color superconductivity is almost unaffected by the presence of a chiral condensate.

In the chiral limit, we find a second order chiral transition at zero chemical potential and a first order chiral transition at zero temperature. Consequently, these meet at a tricritical point at a particular nonzero temperature  $T_{tc}$  and chemical potential  $\mu_{tc}$  as was first discussed in a different phenomenological model in Ref. [7]. We point out that the physics in the vicinity of the tricritical point is described by a  $\phi^6$  theory, and the transition should therefore be characterized by the mean field exponents which we calculate and by logarithmic corrections to scaling [8]. If two-flavor QCD has a second order transition at high temperatures and a first order transition at high densities, then it will have a tricritical point in this universality class. Away from the chiral limit, the second order chiral transition turns into a smooth crossover, while the first order transition remains first order. Of particular interest is the fact that the tricritical point becomes an Ising second order transition. This raises the possibility that even though the pion is massive in nature, long correlation lengths may arise in heavy ion collisions which traverse the chiral transition near  $T_{tc}$  and  $\mu_{tc}$ . Much of the quantitative physics associated with the first order transition is quite model-dependent. However, the physics of the region near the tricritical point is both universal and well-described in mean field theory.

## II. MODELS

Our goal is an exploration of the phase diagram of two flavor QCD in a context which allows us to describe likely patterns of symmetry breaking and to make rough quantitative estimates. As a tractable model, we consider a class of fermionic models for QCD [9] at nonzero temperature and baryon number density [10] where the fermions interact via the instanton-induced interactions between light quarks [6]. In the Euclidean functional integral for the effective action, nonzero temperature  $T$  is implemented via antiperiodic boundary conditions for fermionic fields in the ‘time’ direction with periodicity  $1/T$ . In the presence of a nonvanishing chemical potential  $\mu$  for (net) quark number, the quadratic part of the Euclidean action  $S$  in momentum space reads<sup>3</sup>

$$S_0 = T \sum_{n \in \mathbb{Z}} \int \frac{d^3 \vec{q}}{(2\pi)^3} \bar{\psi}_\alpha^i(q) (\gamma^\nu q_\nu + im + i\gamma^0 \mu) \psi_i^\alpha(q), \quad (1)$$

with an average current quark mass  $m$ . The zeroth component of the momentum  $q \equiv (q^0, \vec{q})$  is discrete with  $q^0(n) = (2n+1)\pi T$  for the fermionic Matsubara modes. Indices  $i = 1, \dots, N_f$  and  $\alpha = 1, \dots, N_c$  denote flavor and color, respectively. Spinor indices are suppressed and

---

<sup>3</sup>We use the Euclidean conventions employed in Ref. [11].

repeated indices are summed. We will write expressions in terms of  $N_f$  and  $N_c$  throughout, even though we will only be concerned with  $N_f = 2$  and  $N_c = 3$  in this paper.<sup>4</sup>

We add a four-fermion interaction to (1) which has the color, flavor and Lorentz structure of the instanton vertex of two-flavor QCD [6]. This interaction properly reflects the chiral symmetry of QCD: axial baryon number is broken, while chiral  $SU(2)_L \times SU(2)_R$  is respected. Color  $SU(3)$  is realized as a global symmetry. One could add other four-fermion interactions that respect the unbroken symmetries of QCD, including in particular that induced by one gluon exchange. We will comment on its effects below. Using the instanton vertex alone is only the simplest way of breaking all the symmetries QCD breaks while respecting those it respects. We note that with the help of appropriate Fierz transformations the instanton interaction can be decomposed into two parts, where one part contains only color singlet fermion bilinears and the other part contains only color  $\bar{\mathbf{3}}$  bilinears:  $S_I = S_I^{(\mathbf{1}_c)} + S_I^{(\bar{\mathbf{3}}_c)}$  with

$$\begin{aligned}
S_I^{(\mathbf{1}_c)} &= G_1 T \sum_{n \in \mathbb{Z}} \int \frac{d^3 \vec{p}}{(2\pi)^3} \left\{ -O_{(\sigma)}[\psi, \bar{\psi}; -p] O_{(\sigma)}[\psi, \bar{\psi}; p] - O_{(\pi)}^a[\psi, \bar{\psi}; -p] O_{(\pi)a}[\psi, \bar{\psi}; p] \right. \\
&\quad \left. + O_{(\eta')}[\psi, \bar{\psi}; -p] O_{(\eta')}[\psi, \bar{\psi}; p] + O_{(a_0)}^a[\psi, \bar{\psi}; -p] O_{(a_0)a}[\psi, \bar{\psi}; p] \right\} , \\
S_I^{(\bar{\mathbf{3}}_c)} &= G_2 T \sum_{n \in \mathbb{Z}} \int \frac{d^3 \vec{p}}{(2\pi)^3} \left\{ -O_{(s)}^{\dagger\alpha}[\bar{\psi}; p] O_{(s)\alpha}[\psi; p] + O_{(p)}^{\dagger\alpha}[\bar{\psi}; p] O_{(p)\alpha}[\psi; p] \right\} . \tag{2}
\end{aligned}$$

Here  $p \equiv (2n\pi T, \vec{p})$  due to the bosonic nature of the fermion bilinears, and  $\dagger$  denotes the operation of Euclidean reflection. The bilinears  $O_{(\sigma)}$ ,  $O_{(\pi)}^a$ ,  $O_{(\eta')}$  and  $O_{(a_0)}^a$  with  $a = 1, 2, 3$  carry the quantum numbers associated with the scalar isosinglet ( $\sigma$ ), the pseudo-scalar isotriplet ( $\pi$ ), the pseudo-scalar isosinglet ( $\eta'$ ) and the scalar isotriplet ( $a_0$ ), respectively. Similarly, the bilinear  $O_{(s)}^\alpha$  ( $O_{(p)}^\alpha$ ), with the color index  $\alpha = 1, 2$  or  $3$ , carries the quantum numbers of the color antitriplet scalar (pseudo-scalar) diquark. (See (3) below for explicit expressions.) The instanton interaction introduces only one coupling. If we take this to be  $G_1$ , then  $G_2 = G_1/(N_c - 1)$  in (2). We have generalized the interaction to allow  $G_1$  and  $G_2$  to take on independent values, although we will always assume that they have the same sign, as for the instanton interaction. We discuss choices of  $G_1$  and  $G_2$  at greater length below. We note from the signs in  $S_I$  that if we choose the sign of  $G_1$  such that the interaction in the  $\sigma$  channel is attractive, so that chiral symmetry breaking is favored, we may expect condensation in the  $\pi$  and scalar diquark channels also. In the chiral limit, one can always make a rotation such that there is no  $\pi$  condensate. A condensate in the pseudoscalar diquark channel would break parity spontaneously, but this seems not to be favored by the interaction (2). We will use the model to explore condensates in the  $\sigma$  and scalar diquark channels.

---

<sup>4</sup>We work throughout with the same chemical potential  $\mu$  for both up and down quarks. Color superconductivity in a system with more down than up quarks, say by about 15% as in a lead or gold nucleus, has been considered in Ref. [12]. The superconductor gap is somewhat reduced, and this suggests that in a heavy ion collision, the system can lower its energy by equalizing the down/up ratio in the densest region of the plasma in order to minimize the gap. This suggests that these dense regions will expel negative pions toward the periphery. [12]

In order to mimic the effects of asymptotic freedom, the interaction has to decrease with increasing momentum. We follow Ref. [1] and implement this via a form factor  $F(\vec{q})$  in momentum space for the three-momenta of each of the fermions, with  $F(0) = 1$  and  $F(\vec{q}) \ll 1$  for  $\vec{q}^2 \gg \Lambda^2$ . Here  $\Lambda$  is some effective QCD cutoff scale which one might anticipate to be in the range  $1/2 - 1$  GeV. With form factors included, the fermion bilinears in the above interaction read

$$\begin{aligned}
O_{(\sigma)}[\psi, \bar{\psi}; p] &= -iT \sum_{n \in \mathbb{Z}} \int \frac{d^3 \vec{q}}{(2\pi)^3} F(\vec{q}) F(\vec{p} - \vec{q}) \bar{\psi}_\alpha^i(-q) \psi_i^\alpha(p - q) , \\
O_{(s)}^\alpha[\psi; p] &= T \sum_{n \in \mathbb{Z}} \int \frac{d^3 \vec{q}}{(2\pi)^3} F(-\vec{q}) F(-\vec{p} + \vec{q}) (\psi^T)_\beta^i(-p + q) C \gamma^5 \epsilon^{\alpha\beta\gamma} \epsilon_{ij} \psi^j_\gamma(-q) , \quad (3)
\end{aligned}$$

for the  $\sigma$  and for the scalar diquark and similarly for the other bilinears.  $C$  denotes the charge conjugation matrix.

### III. THERMODYNAMIC POTENTIAL

The fermionic effective action  $\Gamma$  (the generating functional for  $1PI$  Green functions) determines the field equations that contain all quantum effects. In thermal and chemical equilibrium,  $\Gamma$  depends on the temperature  $T$  and chemical potential  $\mu$ . Here we are interested in a computation of the effective action that determines the field equations for the expectation values of the fermion bilinears  $O_{(\sigma)}[\psi, \bar{\psi}; x]$  and  $O_{(s)}^\alpha[\psi; x]$  whose Fourier components are given in (3). We denote these expectation values by  $\langle \bar{\psi}\psi \rangle$  and  $\langle \psi\psi \rangle$ , respectively. The chiral condensate  $\langle \bar{\psi}\psi \rangle$  is an order parameter for chiral symmetry breaking for vanishing current quark mass  $m$ . For nonzero  $\langle \psi\psi \rangle$ , the diquark bilinear has a color index  $\alpha$  which chooses a direction in color space, thus breaking color symmetry  $SU(3) \rightarrow SU(2)$ .<sup>5</sup> In the following we compute the effective action as a function of the two (space dependent) order parameters.<sup>6</sup> Its behavior for constant order parameters yields the effective potential which corresponds at its extrema to the thermodynamic potential and encodes the equation of state.

For our purposes, it is advantageous to introduce bosonic collective fields into the functional integral which defines the fermionic effective action [13]. These collective fields carry the quantum numbers of the fermion bilinears appearing in (2). We employ a Hubbard-Stratonovich transformation, in which the collective fields are introduced into the functional integral by inserting the identities

<sup>5</sup> The  $U(1)$  of electromagnetism is spontaneously broken but there is a linear combination of electric charge and color hypercharge under which the condensate is neutral which therefore generates an unbroken  $U(1)$  gauge symmetry.

<sup>6</sup>We note that the diquark condensate breaks the gauge symmetry and is therefore not a gauge invariant order parameter. In this respect the situation resembles that in the electroweak sector. As in that case, there is the possibility that a transition associated with a rapid change in physical properties may proceed through a smooth crossover without any thermodynamic singularity.

$$\begin{aligned}
1 &= N \int \mathcal{D}\phi \exp \left\{ -T \sum_{n \in \mathbb{Z}} \int \frac{d^3 \vec{p}}{(2\pi)^3} \left( \frac{\phi(-p)}{2} - O_{(\sigma)}[\psi, \bar{\psi}; -p] G_1 \right) \frac{1}{G_1} \left( \frac{\phi(p)}{2} - G_1 O_{(\sigma)}[\psi, \bar{\psi}; p] \right) \right\}, \\
1 &= \tilde{N} \int \mathcal{D}\Delta^* \mathcal{D}\Delta \exp \left\{ -T \sum_{n \in \mathbb{Z}} \int \frac{d^3 \vec{p}}{(2\pi)^3} \left( \frac{\Delta^{*\alpha}(p)}{2} - O_{(s)}^{\dagger\alpha}[\bar{\psi}; p] G_2 \right) \frac{1}{G_2} \left( \frac{\Delta_\alpha(p)}{2} - G_2 O_{(s)\alpha}[\psi; p] \right) \right\}
\end{aligned} \tag{4}$$

and similar identities for the other bilinears. (Here  $N$  and  $\tilde{N}$  are field independent normalization factors.) The terms quadratic in the fermion bilinears in (4) cancel the original four-fermion interaction (2). As a result, the four-fermion interaction is cast into a Yukawa interaction between fermions and collective fields and a mass term for the collective fields. The fermionic fields then appear only quadratically and can be integrated out exactly, leaving an effective action for the bosonic collective fields alone. We apply a saddle point expansion to the resulting effective action. In particular, standard mean field results correspond to the lowest order in this expansion. Having done the Gaussian integral for the fermions, the saddle point effective action reads

$$\begin{aligned}
\Gamma[\phi, \Delta, \Delta^*; T, \mu] &= -\text{tr} \ln H^{21} - \frac{1}{2} \text{tr} \ln \left[ \mathbf{1} - (H^{21})^{-1} H^{22} (H^{12})^{-1} H^{11} \right] \\
&\quad + T \sum_{n \in \mathbb{Z}} \int \frac{d^3 \vec{p}}{(2\pi)^3} \left[ \frac{1}{4G_1} \phi(-p) \phi(p) + \frac{1}{4G_2} \Delta_\alpha^*(p) \Delta^\alpha(p) \right]
\end{aligned} \tag{5}$$

where, for constant fields  $\phi(x) = \phi$  and (taking the color index  $\alpha = 3$ )  $\Delta_3(x) = \Delta_3^*(x) = \Delta$  and  $\Delta_1 = \Delta_2 = 0$ , the  $H^{ab}$  are diagonal in momentum space:

$$\begin{aligned}
(H^{11})_{ij}^{\alpha\beta}(q, q') &= -C \gamma_5 \epsilon^{\alpha\beta 3} \epsilon_{ij} F(\vec{q})^2 \Delta \delta^3(\vec{q} - \vec{q}') \delta_{n,n'} / 2\pi T = -(H^{22\dagger})_{ij}^{\alpha\beta}(q, q'), \\
(H^{12})_{ij}^{\alpha\beta}(q, q') &= -[C(-\gamma^\mu q_\mu + i\gamma^0 \mu) C + i(m + F(\vec{q})^2 \phi)] \delta^{\alpha\beta} \delta_{ij} \delta^3(\vec{q} - \vec{q}') \delta_{n,n'} / 2\pi T, \\
(H^{21})_{ij}^{\alpha\beta}(q, q') &= [(\gamma^\mu q_\mu + i\gamma^0 \mu) + i(m + F(\vec{q})^2 \phi)] \delta^{\alpha\beta} \delta_{ij} \delta^3(\vec{q} - \vec{q}') \delta_{n,n'} / 2\pi T.
\end{aligned} \tag{6}$$

The integration over the fermions gives rise to a determinant which has been rewritten as the trace of a logarithm in (5). The trace involves the momentum integration as well as the summation over flavor, color and spinor indices. In principle, the saddle point effective action depends on the expectation values of all fermion bilinears occurring in (2). The corresponding collective fields would modify the  $H^{ab}$  of (6) in a straightforward way and for each field a quadratic, mass like, term appears in (5). As discussed in the previous section, these collective fields are not expected to condense. They therefore only contribute to higher order terms in the saddle point expansion.

In this work, we restrict ourselves to the mean field approximation though the approach can be extended to take into account fluctuations around the saddle point. The mean field approximation corresponds to the summation of an infinite class of diagrams, but it is not a systematic expansion in powers of a small parameter. A nonperturbative approach beyond mean field may be performed along the lines of Ref. [11]. There, the two flavor effective potential has been computed at zero baryon density using renormalization group methods. In particular, this approach allows a precise treatment of the effective potential in the vicinity of second order [14,11] or weak first order [15] transitions, both of which we will encounter in Section V. We leave the extension of these methods to nonzero baryon density for future

work, as our goal here is to use mean field results as a qualitative guide in exploring the phase diagram.

We evaluate the effective action in the saddle point approximation for constant field configurations. This yields the effective potential or thermodynamic potential  $\Omega = \Gamma T/V$ . A convenient way to extract the effective potential from (5) is to consider the derivatives of  $\Gamma$  with respect to  $\phi$  and  $\Delta$ . After performing the traces and, in particular, the sums over Matsubara frequencies,  $\Omega$  can be obtained by integration. We find

$$\begin{aligned} \Omega(\phi, \Delta; \mu, T) = & \frac{1}{4G_1}\phi^2 + \frac{1}{4G_2}\Delta^2 \\ & - 2N_F \int_0^\infty \frac{q^2 dq}{2\pi^2} \left\{ (N_c - 2) \left\{ E_\phi + T \ln \left( 1 + \exp \left[ - (E_\phi - \mu)/T \right] \right) \right. \right. \\ & \left. \left. + T \ln \left( 1 + \exp \left[ - (E_\phi + \mu)/T \right] \right) \right\} \right. \\ & + (E_\phi - \mu) \sqrt{1 + F^4 \Delta^2 / (E_\phi - \mu)^2} + (E_\phi + \mu) \sqrt{1 + F^4 \Delta^2 / (E_\phi + \mu)^2} \\ & + 2T \ln \left( 1 + \exp \left[ - (E_\phi - \mu) \sqrt{1 + F^4 \Delta^2 / (E_\phi - \mu)^2} / T \right] \right) \\ & \left. + 2T \ln \left( 1 + \exp \left[ - (E_\phi + \mu) \sqrt{1 + F^4 \Delta^2 / (E_\phi + \mu)^2} / T \right] \right) \right\} + \text{constant} \quad (7) \end{aligned}$$

where  $F(\vec{q})$  is the form factor and

$$E_\phi(\vec{q}) \equiv \sqrt{\vec{q}^2 + (m + F(\vec{q})^2 \phi)^2}. \quad (8)$$

The constant in (7) does not depend on  $\mu$  and  $T$  and is chosen such that the pressure of the physical vacuum is zero. Extremizing  $\Omega$  leads to coupled gap equations for the two order parameters, whose solutions we call  $\phi_0$  and  $\Delta_0$ . That is,

$$\left. \frac{\partial \Omega}{\partial \phi} \right|_{\phi=\phi_0; \Delta=\Delta_0} = \left. \frac{\partial \Omega}{\partial \Delta} \right|_{\phi=\phi_0; \Delta=\Delta_0} = 0 \quad (9)$$

where  $\phi_0$  and  $\Delta_0$  are related to the chiral condensate and the condensate of Cooper pairs by

$$\phi_0 = 2G_1 \langle \bar{\psi} \psi \rangle, \quad \Delta_0 = 2G_2 \langle \psi \psi \rangle. \quad (10)$$

At its extrema, the potential is related to the energy density  $\epsilon$ , the entropy density  $s$ , the quark number density  $n$  and the pressure  $P$  by

$$\Omega(\phi_0, \Delta_0; \mu, T) = \epsilon - Ts - \mu n = -P. \quad (11)$$

Unless otherwise stated, the results we quote in our exploration of the phase diagram are obtained using the smooth form factor

$$F(\vec{q}) = \Lambda^2 / (\vec{q}^2 + \Lambda^2) \quad (12)$$

with  $\Lambda = 0.8$  GeV and with  $G_1 \Lambda^2 = 6.47$  fixed by requiring  $\phi_0 = \phi_0^{\text{vac}} = 0.4$  GeV at  $\mu = T = 0$  in order to obtain a reasonable, albeit qualitative, phenomenology. For most of

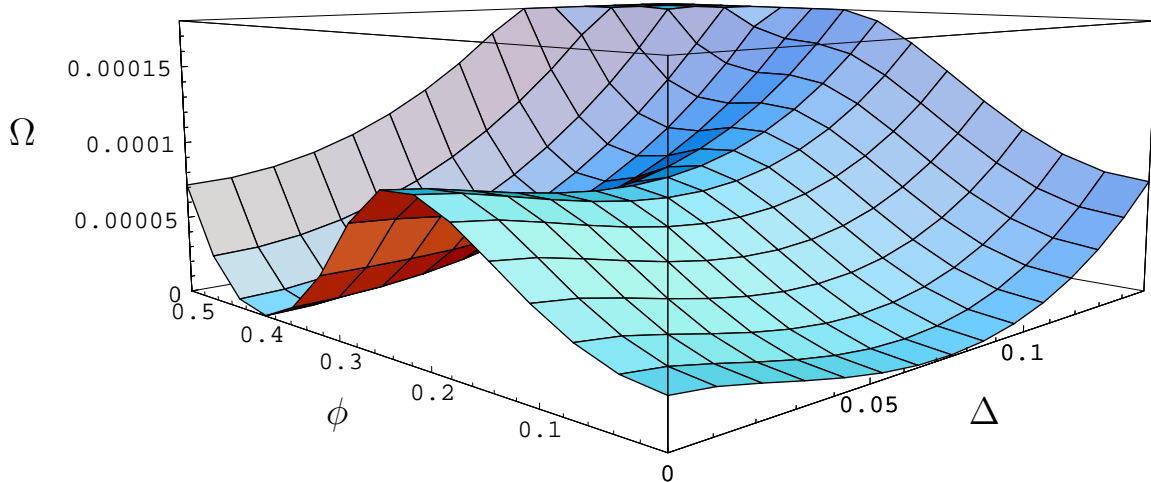


FIG. 1. The thermodynamic potential  $\Omega$  (in  $\text{GeV}^4$ ) as a function of  $\phi$  and  $\Delta$  at  $T = 0$  and  $\mu = 0.292$  GeV. The two degenerate minima have  $\phi = \phi_0^{\text{vac}} = 0.4$  GeV,  $\Delta = 0$  and  $\phi = 0$ ,  $\Delta = 0.072$  GeV.

the discussion we will consider  $G_2 = 3G_1/4$ , which will be motivated at length below. We note that the qualitative features which we address do not depend on this specific choice and we discuss the effects of different choices below.

Although we describe our results in the next sections, it is worth pausing here to emphasize how we use  $\Omega$ . As  $T$  or  $\mu$  or  $m$  changes,  $\Omega$  can have several local minima in the  $(\phi, \Delta)$  plane. The lowest minimum describes the lowest free energy state and is favored. As an example, which we discuss at length in the next section, in Figure 1 we plot  $\Omega(\phi, \Delta)$  at  $T = 0$  and  $\mu = 0.292$  GeV. One observes two degenerate minima corresponding to a first order phase transition at which two phases have equal pressure and can coexist. We discuss the symmetry breaking patterns, their effects and the varied phase transitions which occur as a function of temperature and chemical potential or density in Sections IV–VI.

Before proceeding, we return to our postponed discussion of the appropriate choice for  $G_2/G_1$ , having fixed  $G_1$  phenomenologically. If we take  $G_2$  to be independent of  $G_1$ , there is a phenomenological upper bound which  $G_2$  must satisfy. It is only for  $G_2 < 2G_1$  that the minimum of the potential at  $\mu = T = 0$  has  $\Delta = 0$ . For larger  $G_2$ , color would be spontaneously broken in the vacuum (see also [5]). (As  $G_2$  increases above  $2G_1$ , the vacuum state moves continuously in the  $(\phi, \Delta)$  plane from the  $\Delta = 0$  axis to the  $\phi = 0$  axis.) It is not unreasonable to leave  $G_2$  as a free parameter satisfying  $G_2 < 2G_1$  for the following reason. One could extend our model by introducing four fermion interactions different from (2) with new coupling constants, as long as the correct symmetries are respected. These could again be Fierz transformed into products of fermion bilinears and treated as described above. Assuming that condensation occurs only in the  $\sigma$  and scalar diquark channels, we would end up with a mean field thermodynamic potential precisely of the form (7), but with  $G_1$  and  $G_2$  replaced by rescaled couplings  $G'_1$  and  $G'_2$ . However, there is a caveat if a vector



interaction of the form  $(\bar{\psi}\gamma^\mu\psi)^2$  is present. As with any four fermion interaction, this can rescale  $G_1$  and  $G_2$ . However, because  $\langle\bar{\psi}\gamma^0\psi\rangle = n \neq 0$ , there is an additional qualitative effect. In mean field, the vector interaction translates into an  $n^2$  term added to (7) and an effective shift in the chemical potential proportional to the density  $n$  [10]. We will address the consequences of such an interaction in Section IV.

Suppose that, instead of leaving  $G_2/G_1$  unspecified, we wish to treat the instanton interaction for which  $G_2 = G_1/(N_c - 1)$ . If we could analyze the model without approximation, we would use this ratio. However, the decomposition of the instanton interaction in (2) is, of course, not unique. It can easily be Fierz transformed at the cost of generating products of other bilinears which are, for example, in color octet or **6** representations. Though this is of no concern were we to treat the model exactly, it introduces an ambiguity in the mean field treatment we employ. This is because in addition to generating new bilinears, the Fierz transformation changes the couplings in front of the bilinears in (2). In complete analogy to the above discussion of new interactions, this would change the result (7) for  $\Omega$  by a rescaling of  $G_1$  and  $G_2$ . This ambiguity is a familiar one in studies of chiral symmetry breaking in NJL models, where it is well known that a mean field calculation of the chiral condensate reproduces the results of summing direct and exchange diagrams if one adds to the original interaction a suitably Fierz transformed interaction [10]. Applied to (2), this scales  $G_2$  to zero, removing the diquark bilinears, and introduces color octet terms. This procedure is correct only if no diquark condensate forms, as is of course the case at low densities. Because we are considering the possibility of diquark condensation in addition to chiral condensation, we must then Fierz transform the interaction (including the color octet terms) yet again, this time into a form with  $G_1$  scaled to zero, containing no quark–anti-quark bilinears. Adding this to the interaction without diquark bilinears,<sup>7</sup> we obtain (2) with

$$G_2 = G_1 \frac{N_c}{2N_c - 2} , \quad (13)$$

and with color octet and **6** terms which we now discard because they are assumed not to condense. This procedure yields gap equations which agree, when either  $\phi$  or  $\Delta$  is set to zero, with those obtained previously [1] via extremizing a variational wave function and we use the ratio (13) in all the results we quote unless stated otherwise. The variational method has the advantage of avoiding these ambiguities in the mean field approach we are using here. Our present analysis has the virtue of being tractable at nonzero temperature, for nonzero quark mass and, perhaps most important, in the presence of simultaneous condensation in the  $\sigma$  and scalar diquark channels.

#### IV. ZERO TEMPERATURE PHYSICS

We begin our analysis of the thermodynamic potential (7) at zero temperature and in the chiral limit.  $\Omega(\phi, \Delta; \mu, T)$  is a function of two order parameters. As  $\mu$  changes,  $\Omega$  can

---

<sup>7</sup>This is equivalent to the observation that whereas chiral condensation uses the instanton vertex to turn a  $\bar{u}_L u_R$  into a  $\bar{d}_R d_L$ , condensation in the scalar diquark channel uses it to turn  $u_L d_L$  into  $u_R d_R$ , and so one must add the exchange interaction in this sense also.

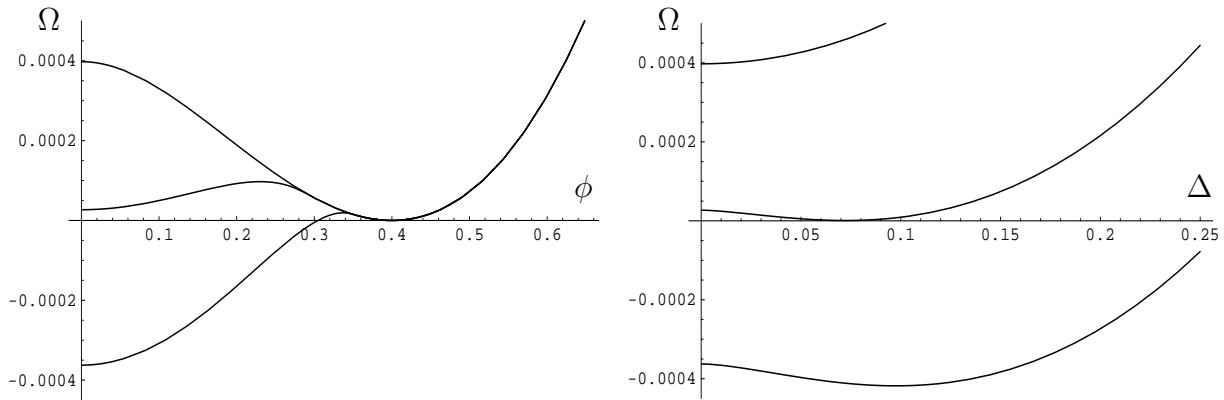


FIG. 2. The zero temperature thermodynamic potential  $\Omega$  (in  $\text{GeV}^4$ ) as a function of  $\phi$  at  $\Delta = 0$  (left panel) and as a function of  $\Delta$  at  $\phi = 0$  (right panel) for several chemical potentials. The curves correspond to (top to bottom)  $\mu = 0, 0.292, 0.35$  GeV. The curves at  $\mu = \mu_0 = 0.292$  GeV are sections of Figure 1.

have several local minima in the  $(\phi, \Delta)$  plane. An example has been given in Figure 1, where for  $\mu = \mu_0 = 0.292$  GeV the potential has two degenerate minima. To see how the potential changes with  $\mu$ , in Figure 2 we display sections of the  $(\phi, \Delta)$  plane for  $\Delta = 0$  and  $\phi = 0$  respectively. Let us first focus on the left panel. At  $\mu = 0$ ,  $\Omega$  has a minimum at  $\phi = 0.4$  GeV. As  $\mu$  is increased,  $\Omega$  at this minimum is unchanged. Since

$$n = -\frac{\partial\Omega}{\partial\mu} \text{ at fixed } T, \phi = \phi_0, \Delta = \Delta_0, \quad (14)$$

we conclude that the phase described by this minimum has baryon density zero, as we expect for the vacuum. As  $\mu$  is increased sufficiently, a second local minimum of  $\Omega$  develops with  $\phi = 0$  and  $\Delta \neq 0$ . The system remains in the vacuum state with density zero and  $\phi_0$  unchanged until the chemical potential is increased to  $\mu = \mu_0$  where both minima become degenerate with  $\Omega = -P = 0$  as seen in Figure 1. There is now a zero pressure chirally symmetric color superconductor phase whose density we denote  $n_0$  which has the same  $\mu$  and  $P$  as the vacuum phase. Before  $\mu$  can be increased any further, the system must undergo a first order phase transition during which the density increases from zero to  $n_0$ . At all intermediate densities, the system is in a mixed phase in which there are regions with density  $n_0$  and regions of vacuum. Once the transition is complete,  $\mu$  can increase further, and the lowest  $\Omega$  configuration becomes one with  $\Omega < 0$ , that is with positive pressure, in which  $n > n_0$ . In the top panels of Figure 3, we show the behavior of the global minimum  $(\phi_0, \Delta_0)$  of  $\Omega$  and the density as a function of  $\mu$ . We have verified that there are no other minima, for example with both  $\phi$  and  $\Delta$  nonzero, as long as we stay in the chiral limit. The locations of the extrema of the curves in Figure 2 agree with those obtained in Ref. [1] and described also in Ref. [16]. Treating the full problem, one observes that the first order phase transition does in fact occur between the two minima in Figure 1, at  $\mu = \mu_0 = 0.292$  GeV.

There is an interesting interpretation of this zero temperature first order phase transition [1,16,17]. For reasonable choices of parameters,  $n_0$  is greater than nuclear matter density

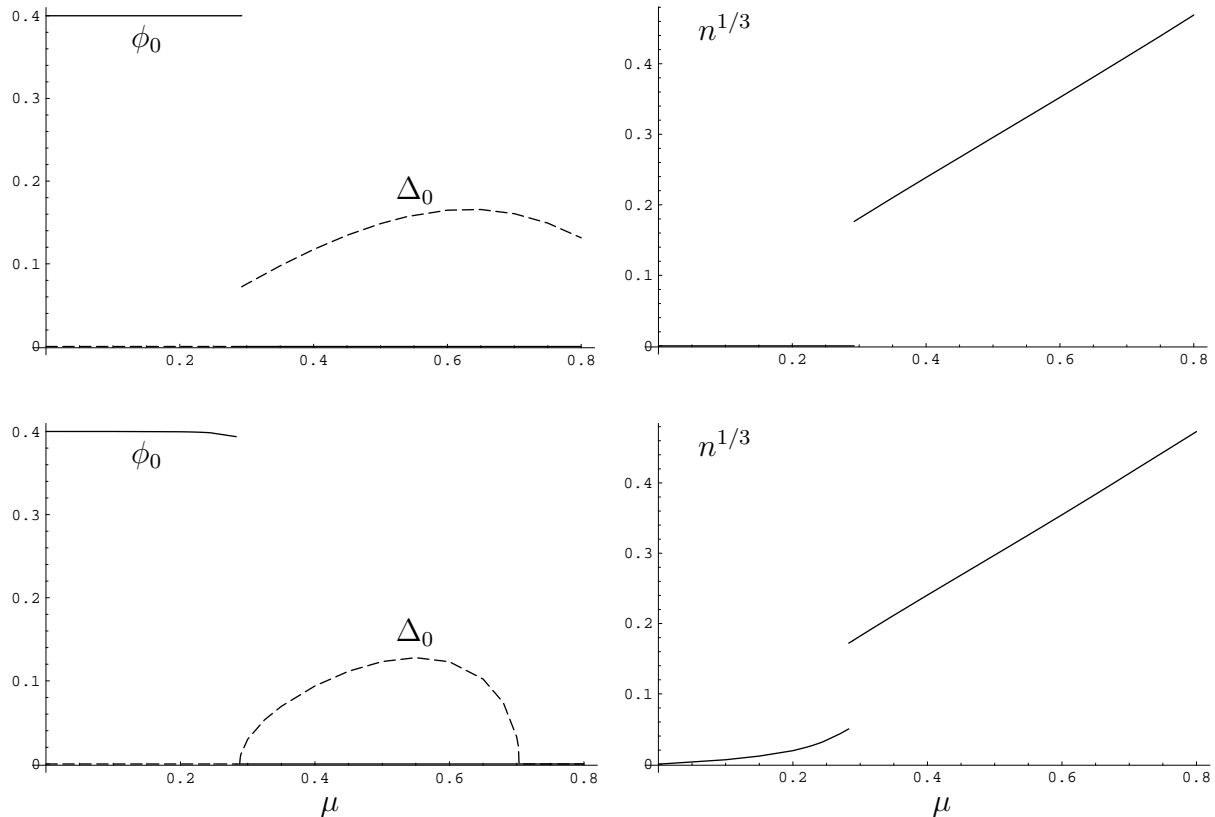


FIG. 3. Left panels show  $\phi_0$  and  $\Delta_0$  (namely  $\phi$  and  $\Delta$  at the global minimum of  $\Omega$ ) as functions of  $\mu$  for  $T = 0$  (above) and  $T = 0.03$  GeV (below). The right panels show the quark number density  $n$  for the same parameters. We describe the results at nonzero temperature in the next section.

and comparable to the baryon density in a *nucleon*.<sup>8</sup> Ordinary nuclear matter is then in the mixed phase of this transition and consists of nucleon sized droplets within which  $n = n_0$  and  $\phi = 0$ , surrounded by regions of vacuum. Although it is nice to see that the model forces quarks to be located within droplets within which they have zero mass, the model must obviously be extended in several respects. First, a short range repulsion between droplets must be included, so that small droplets are favored over bigger ones [16]. Second, color must be gauged if the model is to yield droplets which are color singlets. It is crucial to this interpretation that  $\mu_0 < \phi_0^{\text{vac}}$ . In the chiral limit,  $\phi_0$  corresponds to the constituent quark mass and therefore if  $\mu$  is increased above  $\phi_0^{\text{vac}}$  the (formerly) vacuum phase becomes populated with a gas of constituent quarks. If  $\mu_0 < \phi_0^{\text{vac}}$ , the first order transition to the high density phase which occurs at  $\mu = \mu_0$  preempts this. Within the present model,  $\mu_0 < \phi_0^{\text{vac}}$

---

<sup>8</sup>If we identify  $n_0$  with the quark number density in a nucleon and take this to be three times that in nuclear matter, we should require  $n_0^{1/3} = 0.22$  GeV. The choice of parameters we are using for illustration yields a smaller value  $n_0^{1/3} = 0.18$  GeV in the chiral limit, as seen in Figure 3. We shall see in Section VI that we obtain  $n_0^{1/3} = 0.22$  GeV for a quark mass of 10 MeV.

only for  $\Lambda < 2.2$  GeV. Furthermore, adding a four fermion interaction to model one gluon exchange introduces an effective shift in  $\mu$  as discussed in Section III, and this increases the value of  $\mu_0$  [10]. With vector interactions included, one can construct models with reasonable values of a suitably defined  $\Lambda$  in which  $\mu_0 > \phi_0^{\text{vac}}$  [10]. In such a model, the first order transition occurs between a gas of constituent quarks with a nonzero density  $n_-$  and a gas of massless quarks with a density  $n_+ > n_-$ , and  $n_-$  can be greater than nuclear matter density for reasonable choices of parameters. If one then gauges color, the gas of constituent quarks which the model describes at densities below  $n_-$  is expected to become a gas of baryons. We now turn to nonzero temperature and one of the things which we will see is that models with  $n_- = 0$  and with  $n_- > 0$  are less different than they appear to be at zero temperature.

## V. THE PHASE DIAGRAM

In Figure 4, we present the phase diagram of the model as a function of  $\mu$  and  $T$ , and as a function of  $n$  and  $T$ . We devote this section to a discussion of the physics shown in these figures. Let us first focus on Figure 4a, and ignore the quark number density  $n$ . We find that at  $\mu = 0$ , the chiral phase transition as a function of increasing temperature is second order. In our present mean field treatment, it is of course a mean field transition. A second order chiral phase transition in two flavor QCD at nonzero temperature has the appropriate symmetry to be in the  $O(4)$  universality class [18–21], and a treatment of the present model which went beyond mean field theory, like that in Ref. [11], would find critical exponents characteristic of this universality class. There is no reason to expect a small chemical potential to change this result, since this introduces no new massless degrees of freedom in the effective three dimensional theory which describes the long wavelength modes near  $T = T_c$ . This argument has been made at greater length in Ref. [22]. However, it is possible that as a parameter in the theory is changed, the quartic coupling in the effective three dimensional theory can become negative, making the transition first order. Where the quartic coupling is zero, one has a tricritical point. (This is precisely what is expected to occur at  $\mu = 0$  at a particular value of the strange quark mass. [19–21,23]) Since we have seen that the zero temperature, nonzero  $\mu$  transition is first order and we have found a second order transition at high temperature, we expect and find a tricritical point where the second order transition becomes first order. The tricritical point occurs at  $\mu = \mu_{\text{tc}} = 211$  MeV and  $T = T_{\text{tc}} = 101$  MeV for the parameters we are using.

We have verified that at the tricritical point  $\Omega \sim \phi^6$  as we expect, based on the arguments above.<sup>9</sup> In the vicinity of the tricritical point,  $\Omega$  therefore has the form

$$\Omega(\phi, 0; \mu, T) = \Omega(0, 0; \mu_{\text{tc}}, T_{\text{tc}}) + \frac{a(\mu, T)}{2}\phi^2 + \frac{b(\mu, T)}{4}\phi^4 + \frac{c(\mu, T)}{6}\phi^6 - h\phi, \quad (15)$$

where the coefficient  $h$  of the linear term is proportional to the current quark mass. The coefficients  $a$  and  $b$  are both zero at the tricritical point, and barring accidental cancellations

---

<sup>9</sup>In fact,  $\Omega(\phi, \Delta = 0; \mu_{\text{tc}}, T_{\text{tc}}) = 0.033\phi^6 - 0.000392$ , all in GeV.

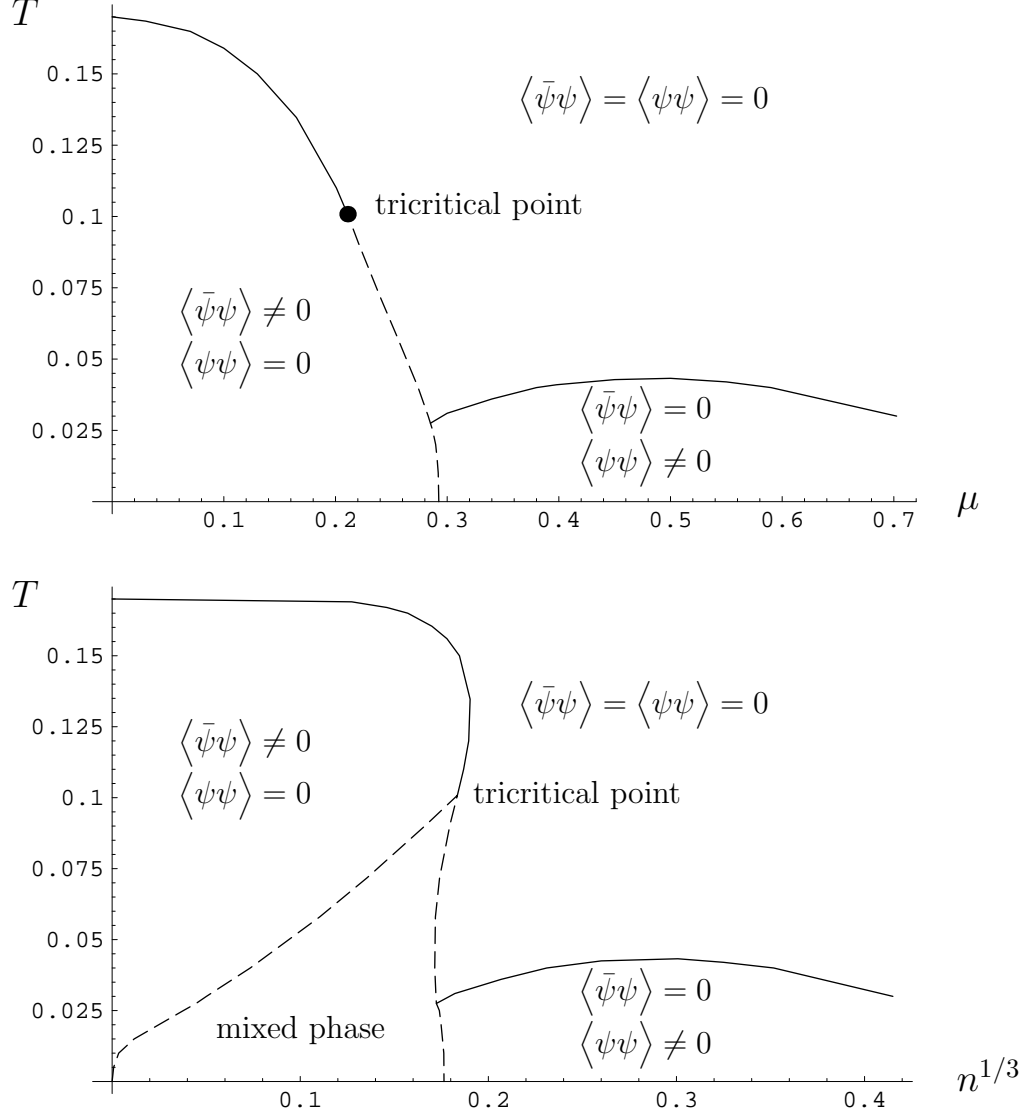


FIG. 4. Phase diagram as a function of  $T$  and  $\mu$ , and as a function of  $T$  and  $n^{1/3}$  (all in GeV). This section can be viewed as one long caption for these figures. The solid curves are second order phase transitions; the dashed curves describe the first order transition.

both will be linear in both  $(T - T_{tc})$  and  $(\mu - \mu_{tc})$ . The  $\mu$  and  $T$  dependence of  $c$  is not important, as  $c$  does not vanish at the tricritical point, and it is convenient to set  $c = 1$ . It is easy to verify that, near the tricritical point, the line of second order transitions is given by  $a = 0, b > 0$  and the line of first order transitions is given by  $a = 3b^2/16, b < 0$ . Minima of  $\Omega$  are described by the scaling form

$$h = \phi_0^5 \left( \frac{a}{\phi_0^4} + \frac{b}{\phi_0^2} + 1 \right). \quad (16)$$

From this, we read off the exponents  $\delta = 5$ ,  $1/\beta = 4$ , and  $\phi_t/\beta = 2$  where  $\phi_t$  is called the crossover exponent because tricritical (as opposed to first or second order) scaling is observed for  $b < a^{\phi_t}$ . For more details see Refs. [8,21]. The relation between  $a$  and  $b$  and  $(T - T_{tc})$  and  $(\mu - \mu_{tc})$  depends on the slope of the line of phase transitions which end at

the tricritical point in Figure 4a and is not universal. In general, our model should not be used quantitatively. However, if we trust the qualitative feature that the transition is second order at high temperatures and first order at low temperatures, then QCD with two flavors will have a tricritical point in the same universality class as that in our model. Since  $d = 3$  is the critical dimension for  $\phi^6$  theory, we expect that a complete treatment would yield mean field exponents in agreement to those in our model, although there would be logarithmic corrections to the scaling law (16) [8]. The reason we have described the physics of the tricritical point carefully is that, because we have a  $\phi^6$  theory in three dimensions, the universal critical exponents will be given quantitatively by those we find in mean field theory.

At low temperatures, one has color superconductivity at chemical potentials immediately above the first order phase transition. However, the superconducting order parameter  $\Delta$  is reduced by nonzero temperature, as shown in Figure 3. In Figure 4 we see that for the parameters we are using, color superconductivity persists up to temperatures as high as 45 MeV for the most favorable chemical potential. The energy gap in the color superconductor phase (that is, the energy to create a quasiparticle–quasihole pair) is  $2\Delta_0 F(\mu)^2$ . BCS theory predicts that, at weak coupling, the critical temperature  $T_c^\Delta$  at which the superconductivity vanishes should be given by  $0.57F(\mu)^2\Delta_0(T = 0)$ . Our results are within a few percent of this. This suggests that  $T_c^\Delta$  is sensitive to the shape of the form factor. For example, we have verified that if we use a form factor with a sharp cutoff we can easily increase  $T_c^\Delta$  by a factor of two, although this tends to increase  $T_c$  for the finite temperature transition at zero chemical potential also. If we generalize beyond the instanton interaction, and therefore do not require (13) but simply impose  $G_2 < 2G_1$  as required if color  $SU(3)$  is to be a symmetry of the vacuum, then we find that values of  $\Delta_0$  and  $T_c^\Delta$  can arise which are up to four times larger than those we show in our figures.

The transition at nonzero temperature at which color superconductivity is lost is second order in our model. Because of the shape of the  $T_c^\Delta$  curve as a function of  $\mu$ , there are temperatures (like  $T = 30$  MeV in Figure 3) for which, as  $\mu$  is increased, one first completes the first order chiral transition, then has a region with  $\phi_0 = \Delta_0 = 0$ , then has a second order transition to a color superconducting phase, before finally having another second order transition to a phase with no condensates. If one neglects gluons, one could study this second order transition by doing a renormalization group analysis to first determine whether there is a second order transition as in our mean field analysis, and then to determine the universal exponents due to the long wavelength fluctuations of  $\Delta$ , associated with the breaking of the global color symmetry. We expect, however, that the second order nature of the transition at  $T = T_c^\Delta$  can change once gauge fields are introduced. For example, the electroweak phase transition is second order when only the Higgs field is included, but can be either first order or a smooth crossover once gauge fields are taken into consideration. We leave a Ginzburg-Landau treatment of the physics near  $T_c^\Delta$  (including both gluons and the superconductor order parameter  $\Delta$ ) to future work.

By not showing  $n$ , Figure 4a obscures important features seen in Figure 4b, including for example the fact (as discussed above) that at zero temperature, one of the phases in equilibrium at the first order transition has zero density. At any nonzero temperature which is low enough that the transition is first order, the transition occurs between a gas of constituent quarks with density  $n_-$  and a gas of massless quarks with density  $n_+$ . In other

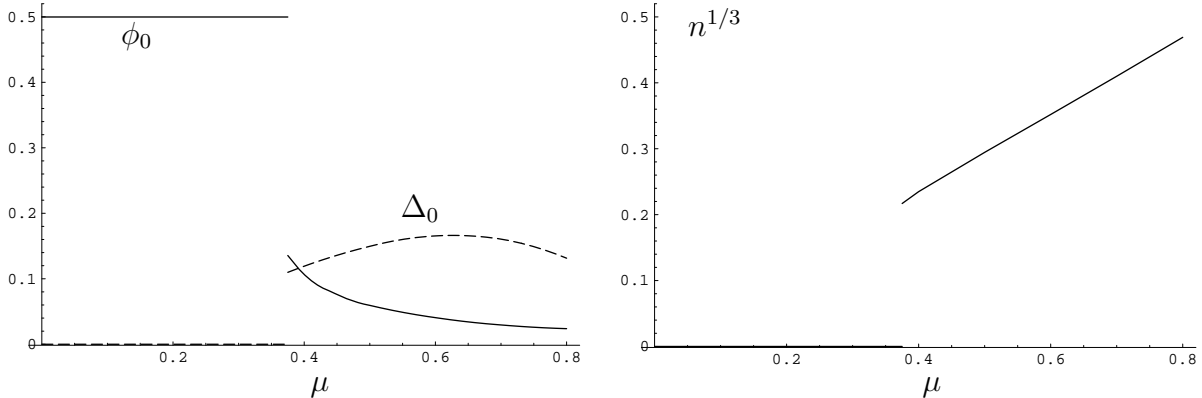


FIG. 5. As for Figure 3 at zero temperature, but with a current quark mass  $m = 10$  MeV. We observe coexisting  $\phi_0 \sim \langle \bar{\psi}\psi \rangle$  and  $\Delta_0 \sim \langle \psi\psi \rangle$  condensates in the high density phase.

words, in the mixed phase one has droplets containing massless quarks as before, but they are now surrounded by a dilute gas of constituent quarks, rather than by vacuum. Once gluons are introduced, both the droplets of the  $n = n_+$  phase and the constituent quarks in the low density phase are expected to form color singlets. Thus, the description of baryons as droplets is less complete at nonzero temperature than at zero temperature.

It is clear that there is no model-independent significance to the dashed lines in Figure 4b which mark the boundaries of the mixed phase. In nature, with gluons and with repulsive short range interactions between nucleons, the only curve which can be defined is the one which bounds the region in which chiral symmetry is broken. Locating this boundary requires further analysis of the first order transition, but it seems likely [1,16,24] that it is associated with the percolation of the droplets of the high density phase. More precisely, once one no longer has regions of the low density phase (with nonzero  $\phi_0$ ) which are of infinite extent, chiral symmetry will be restored. Thus, the density at which chiral symmetry is restored must be somewhat to the left of  $n_+$ . Similarly, color superconductivity sets in at densities above which there are regions of the high density phase of infinite spatial extent. Chiral symmetry restoration is associated with the “unpercolation” of the low density phase, while the onset of color superconductivity is associated with the percolation of the dense phase, and both occur at densities somewhat below  $n_+$ . None of this physics is visible in Figure 4a, since it all occurs within the mixed phase region. It is important to realize, therefore, that if one is interested in the experimentally relevant question of whether or not a first order transition occurs as  $n$  is increased above nuclear matter density, this analysis does not provide an answer. The percolation transition could be smooth or second order, even though it is occurring “within” the first order phase transition described by the model. What is robust, and as we shall see in the next section may be quite significant, is that regardless of how the physics as a function of  $n$  works within the mixed phase region, there is a tricritical point in the phase diagram.

## VI. PHYSICS AWAY FROM THE CHIRAL LIMIT

In the previous section, we have explored the phase diagram at nonzero temperature and baryon density in the chiral limit. We now turn on a small but nonzero quark mass  $m$ , as in nature. We see from Figure 5 that in the low temperature phase, the quark mass affects  $\phi_0$ , but leaves  $\Delta_0 = 0$ . We observe that  $\phi_0^{\text{vac}}$ ,  $\mu_0$  and the critical temperature for the chiral transition at zero density all increase with  $m$ . One might reasonably choose to reduce  $G_1$  as  $m$  is increased in order to keep  $\phi_0^{\text{vac}}$  fixed. With  $G_2/G_1$  fixed, this would reduce  $G_2$  and would therefore reduce  $\Delta_0$ . We do not do this because our goal is to find any effects of the presence of the chiral condensate on the superconductor condensate and we do not wish these effects to be entangled with the effects of a reduction in  $G_2$ . In the phase with density  $n_0 = (0.217 \text{ GeV})^3$  attained immediately upon completion of the phase transition, both condensates have comparable magnitudes with  $\phi_0 = 0.136 \text{ GeV}$  and  $\Delta_0 = 0.110 \text{ GeV}$ . We observe only a very small dependence of  $\Delta_0$  on  $m$ , as long as the constituent quark mass  $m + \phi_0$  is smaller than  $\mu$ . (Compare Figure 5 to Figure 3, where  $m = 0$ .) This insensitivity can be understood by noting that although the Cooper pairs have low momentum, they are formed from quarks which have momenta close to the Fermi surface. Adding a quark mass  $m \ll \mu$  does not significantly affect the density of states or the interactions of the quasiparticles with momenta of order  $\mu$ . This is consistent with our finding that the temperature  $T_c^\Delta$  at which the superconductivity is lost is almost unchanged.

The phase transition at  $T = T_c^\Delta$  remains second order in the presence of a nonzero quark mass. This result can be understood by expanding the effective potential at small  $\phi$  and  $\Delta$ . Whereas a quark mass adds a term to the effective potential which is linear in  $\phi$  at small  $\phi$ , it does not introduce a term linear in  $\Delta$ . It can modify the coefficient of the  $\Delta^2$  term, which changes the critical temperature for the transition but leaves it second order.

To conclude our discussion of color superconductivity, we remark that the phenomenon seems quite robust. It is not significantly disturbed by the simultaneous presence of a chiral condensate as long as the constituent quark mass is less than the chemical potential. Although the phenomenon is robust, our estimate of the critical temperature at which it vanishes is less so. For the parameters we have used for illustrative purposes,  $T_c^\Delta$  is 30–45 MeV, but changes in the form factor can double this and phenomenologically acceptable changes in the coupling constant  $G_2$  can multiply  $T_c^\Delta$  by up to a factor of four. A definitive answer of whether or not color superconductivity can arise in heavy ion collisions, in which the necessary densities are likely accompanied by temperatures of order 100 MeV, must await a less qualitative treatment.

Our model reveals the possibility of a tricritical point in the phase diagram for two-flavor QCD in the chiral limit. Physics in the vicinity of the tricritical point is described by a  $\phi^6$  field theory, whose critical exponents are given quantitatively by the mean field analysis in this paper. What, then, happens in this region of temperature and chemical potential in the presence of a small quark mass? It is well known that a nonzero quark mass does have a qualitative effect on the second order transition which occurs at temperatures above  $T_{\text{tc}}$ . This  $O(4)$  transition becomes a smooth crossover, because terms linear in  $\phi$  now arise in  $\Omega$ . A small quark mass cannot eliminate the first order transition below  $T_{\text{tc}}$ . Therefore, whereas we previously had a line of first order transitions and a line of second order transitions meeting at a tricritical point, with  $m \neq 0$  we now have a line of first order transitions ending



at an ordinary critical point, as in the liquid-gas phase diagram. At this critical point, one degree of freedom (that associated with the magnitude of  $\phi$ ) becomes massless, while the pion degrees of freedom are massive since chiral symmetry is explicitly broken. Therefore, this transition is in the same universality class as the three-dimensional Ising model.

From many studies of QCD at nonzero temperature, we are familiar with the possibility of a second order transition, with infinite correlation lengths, in an unphysical world in which there are two massless quarks. It is exciting to realize that if the finite density transition is first order at zero temperature, as in the models we have considered, then there is a tricritical point in the chiral limit which becomes an Ising second order phase transition in a world with chiral symmetry explicitly broken. In a sufficiently energetic heavy ion collision, one may create conditions in approximate local thermal equilibrium in the phase in which spontaneous chiral symmetry breaking is lost. Depending on the initial density and temperature, when this plasma expands and cools it will traverse the phase transition at different points in the  $(\mu, T)$  plane. Our results suggest that in heavy ion collisions in which the chiral symmetry breaking transition is traversed at baryon densities which are not too high and not too low, a very long correlation length in the  $\sigma$  channel and critical slowing down may be manifest even though the pion is massive.

#### ACKNOWLEDGMENTS

We are especially grateful for discussions with M. Alford and F. Wilczek and thank R. L. Jaffe, D.-U. Jungnickel, J. W. Negele, D. T. Son, M. Stephanov and C. Wetterich for very useful conversations.

## REFERENCES

- [1] M. Alford, K. Rajagopal and F. Wilczek, hep-ph/9711395, to appear in Phys. Lett. **B**.
- [2] R. Rapp, T. Schaefer, E. V. Shuryak and M. Velkovsky, hep-ph/9711396.
- [3] D. Bailin and A. Love, Phys. Rept. **107** (1984) 325, and references therein.
- [4] M. Iwasaki and T. Iwado, Phys. Lett. **B350** (1995) 163.
- [5] D. Diakonov, H. Forkel and M. Lutz, Phys. Lett. **B373** (1996) 147.
- [6] G. 't Hooft, Phys. Rev. **D14** (1976) 3432.
- [7] A. Barducci, R. Casalbuoni, S. De Curtis, R. Gatto and G. Pettini, Phys. Lett. **B231** (1989) 463; Phys. Rev. **D49** (1994) 426.
- [8] For a review, see I. Lawrie and S. Sarbach in *Phase Transitions and Critical Phenomena* **9** (1984) 1, ed. C. Domb and J. Lebowitz (Academic Press).
- [9] Y. Nambu and G. Jona-Lasinio, Phys. Rev. **122** (1961) 345; **124** (1961) 246.  
V. G. Vaks and A. I. Larkin, Sov. Phys. JETP **13** (1961) 192.
- [10] For reviews, see S. P. Klevansky, Rev. Mod. Phys. **64** (1992) 649, and T. Hatsuda and T. Kunihiro, Phys. Rept. **247** (1994) 221.  
Studies of finite density physics in Nambu Jona-Lasinio models include: V. Bernard, U.-G. Meissner and I. Zahed, Phys. Rev. **D36** (1987) 819; T. Hatsuda and T. Kunihiro, Phys. Lett **B198** (1987) 126; M. Asakawa and K. Yazaki, Nucl. Phys. **A504** (1989) 668; S. Klimt, M. Lutz and W. Weise, Phys. Lett. **B249** (1990) 386; M. Lutz, S. Klimt and W. Weise, Nucl. Phys. **A542** (1992) 521; D. Ebert *et al*, Int. J. Mod. Phys. A **8** (1993) 1295; S. Ying, Phys. Lett. **B283** (1992) 241.
- [11] J. Berges, D. Jungnickel and C. Wetterich, hep-ph/9705474.
- [12] M. Alford, K. Rajagopal and F. Wilczek, hep-ph/9802284, to appear in the proceedings of Quark-Matter '97.
- [13] Similar bosonization techniques can be found in R. Alkofer and H. Reinhardt, *Chiral Quark Dynamics*, Springer 1995, and references therein.
- [14] J. Berges, N. Tetradis and C. Wetterich, Phys. Rev. Lett. **77** (1996) 873.
- [15] J. Berges and C. Wetterich, Nucl. Phys. **B487** (1997) 675.
- [16] K. Rajagopal, hep-ph/9803341, talk given at Yukawa International Seminar, Kyoto, 1997, to appear in Prog. T. Phys.
- [17] See also M. Buballa, Nucl. Phys. **A611** (1996) 393.
- [18] R. Pisarski and F. Wilczek, Phys. Rev. **D29** (1984) 338.
- [19] F. Wilczek, Int. J. Mod. Phys. **A7** (1992) 3911.
- [20] K. Rajagopal and F. Wilczek, Nucl. Phys. **B399** (1993) 395.
- [21] For a review, see K. Rajagopal, Quark-Gluon Plasma 2, (1995) 484, ed. R. Hwa.
- [22] S. Hsu and M. Schwetz, hep-ph/9803386.
- [23] S. Gavin, A. Gocksch and R. Pisarski, Phys. Rev. **D49** (1994) 3079.
- [24] Previous percolation-based approaches to the chiral transition as a function of density include: G. Baym, Physica **96A** (1979) 131; T. Celik, F. Karsch and H. Satz, Phys. Lett. **97B** (1980) 128.